

Fault Ride through technique in Doubly Fed Induction Generator based Wind Turbines

N.Manonmani

Assistant professor, EEE Sri Krishna College of Engineering and Technology
Coimbatore, India
manonmani@skcet.in 9994886364

Abstract

The increasing concerns over climate change and fossil fuel depletion leads renewable energy sources for electricity generation. Therefore, wind turbines are increasing in popularity, along with doubly-fed induction machines (DFIGs) used in generation mode. Present grids codes require DFIGs to provide voltage support during a grid fault. The Fault Ride-Through (FRT) capability of DFIGs is the focus of this project, in which modifications to the DFIG controller have been proposed to improve the FRT capability. The Static Synchronous Compensator (STATCOM) controller has been applied with proposed method to study its influence on the voltage at the Point of Common Coupling (PCC). The proposed method was compared with other FRT capability improvement methods. The simulation of the dynamic behavior of DFIG-based wind turbines during grid fault is simulated using MATLAB/ Simulink. The result obtained clearly demonstrates the efficiency of the proposed method.

Keywords—Fault ride through (FRT), Doubly fed Induction generator, STATCOM, Grid code.

I. INTRODUCTION

Wind is the most popular renewable energy resources [1]. In 2013, a wind turbine and wind farm database of more than 50 countries around the world was published [2], showing the percentage of wind energy generated between 1997 and 2013, was increased. In the past, simple squirrel-cage-induction generator-based wind turbines were directly connected to a three-phase power system and the rotor of the turbine was connected to the shaft of the generator through a fixed gear box. However, this type of generator had to operate at a fixed wind speed, which is found to be impractical. In response to this limitation, some induction generators were developed to use pole-adjustable winding configurations in order to operate at variable wind speeds. Nowadays, many modern and large wind turbines use Adjustable-Speed Generators (ASGs). The main advantages over Fixed-Speed Generators (FSGs) are that mechanical stress is reduced, power quality is improved, and the system efficiency is increased. The most common type of ASGs used to produce electricity in wind turbines is The Doubly-Fed Induction Generator (DFIG) [4].

The behavior of DFIGs during grid disturbances like short-circuit faults has been the focus of numerous studies. In the past, the majority of national network operators do not require that wind farms must be connected to the grid during grid

disturbances. However, due to an increase in wind farms, it is now mandatory for wind turbines to be connected to the grid during disturbances, in order to support it with reactive power [7]. Fault Ride Through (FRT) or Low Voltage Ride Through (LVRT) along with other methods and techniques have been developed to improve the FRT capability of DFIGs during fault periods.

Active crowbars are commonly used to protect the rotor-side converters (RSCs) against current and voltage transients, which are caused due to voltage sags in the stator side [3], [4]. When a fault occurs, this active crowbar is engaged and the DFIG behaves as an induction machine since the rotor winding is short circuited by the shunt resistors and the RSC is disabled. The main disadvantage of crowbar protection is that the DFIG consumes more reactive power when it is activated and during a fault this provokes the grid voltage dip. Series dynamic resistors are utilized [5] to control significant rotor currents so that the rotor circuits and RSC can be effectively protected by the coordination control of the crowbar and the chopper resistor. However, if the wind farm is connected to a weak power network, the employment of such techniques makes the DFIG unable to supply essential amounts of reactive power, and thus increases the chance of system instability.

Hence, a new modification of the RSC was applied by combining electromagnetic torque, current and voltage controller. Furthermore, the research modeled a Flexible AC Transmissions System (FACTS), one of the most widely used reactive power sources. Here, FACTS was used to generate and observe the reactive power required at the PCC. Subsequently, the proposed FACTS controller with FRT capability was compared to FRT capability with crowbar controller. It was reported that, when using the crowbar method, undesirable fluctuations of electromagnetic torque most likely occur. To solve this problem, one of the FACTS device static synchronous compensators (STATCOMs) have been proposed to supply additional reactive power and compensate the DFIG consumption [6].

II. THE DOUBLY FED INDUCTION GENERATOR WIND TURBINE

An overview of the theory and principles of DFIG operation and control. The aim is to cover the necessary background to analyze the fault response of a conventional wind turbine DFIG. Double-fed induction generators are preferable in wind turbine applications that require a constant output power,

system frequency at various speeds of the generator shaft. DFIGs are electric generators that have windings on both stator and rotor sides. The stator is directly connected to the grid and the rotor is connected to the grid via a power converter, as shown in Fig.1. Furthermore, the voltage on the stator is supplied from the power system and the voltage on the rotor is induced by the power converter, the generated electrical power is supplied to the grid through both the stator and the rotor. The DFIG has three inputs: the stator voltage, the rotor voltage, and the mechanical angular speed of the generator's rotor. It also has three outputs: the induced stator, the rotor currents, and the electromagnetic torque, as shown in Fig.1. The next sections provide a brief description of DFIG theory and equations.

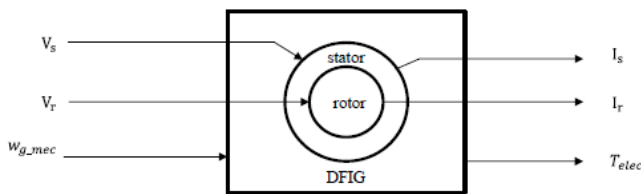


Fig. 1. DFIG block with inputs and outputs

A. The Classic Configuration Of A DFIG-Based Wind Turbine

In most instances, generating electricity from wind turbines is a two-stage process. In the first stage, the turbine rotor (prime mover) converts kinetic energy from the wind into mechanical rotational power. In the second stage, a generator converts mechanical power into electrical power. There are presently two options for coupling a turbine rotor to a generator shaft. One option, which is the most popular, involves coupling the two components physically via a gearbox. The other option is to connect the rotor directly to the generator. In the case considered, the type of generator is a DFIG, where the stator is directly connected to the grid and the rotor winding is connected to the grid via a back-to-back voltage source converter (BVSC). A common configuration of a DFIG-based wind turbine is illustrated in Fig.2. In the next section, a model of a wind turbine is introduced.

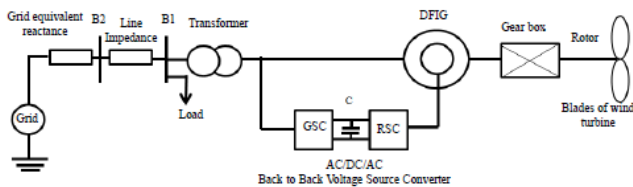


Fig.2. Conventional wind turbine configuration with a feinducti-generator

B. The Basic Concept of DFIG

As illustrated in Fig.2, when the stator is supplied by the grid voltage of frequency, the stator flux is induced and will rotate at a constant speed, which is known as synchronous speed.

Consequently, and according to Faraday's law, the stator flux will induce an electromotive force in the rotor windings. This, together with the injected voltage from the power converter to the rotor windings, will induce the rotor current, which also produces a rotating rotor flux. Similarly, this rotating rotor flux will induce the electromotive force in the stator windings, which induces a current in the stator windings. The equivalent circuit for steady state of DFIG is illustrated in Fig.3.

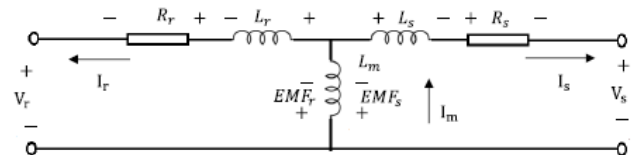


Fig. 3. One-phase equivalent circuit for steady state of DFIG

where

- $R_s R_r$: the stator, rotor resistance
- $L_s L_r$: the stator, rotor leakage inductance
- L_m : the mutual inductance
- $I_s I_r$: the stator, rotor-induced current
- EMFs EMF_r : the stator, rotor electromotive force induced

The voltages and currents in the rotor windings rotate at a speed which is known as the electrical rotor angular velocity (ω_r). Likewise, the voltages and currents in the stator windings rotate at the electrical stator angular velocity (ω_s). The relation between ω_r and ω_s is given as follows:

In addition, the relation between ω_s and ω_{g_elec} is commonly called the slip (s). By combining this relation with Eq. 1, the relation between ω_r and ω_s is expressed in Eq. 2.

$$\omega_r = \omega_s - \omega_{g_elec} \tag{1}$$

$$\omega_{g_elec} = \omega_{g_mec} * p \tag{2}$$

$$slip(s) = \frac{\omega_s - \omega_{g_elec}}{\omega_s} \tag{3}$$

$$\omega_r = s \omega_s \tag{4}$$

$$f_r = s f_s \tag{5}$$

$f_s f_r$: the stator, rotor frequency

The sign of the slip determines the mode of the DFIG operation, either in a sub-synchronous operation or hyper-synchronous operation, as well as the receiving or supplying the power.

According to various models of DFIGs established by numerous authors, the space vectors of the machine are represented by different reference frames in order to create a dynamic model of a DFIG. Examples of these frames are the stator reference frame, the rotor reference frame, and the synchronous reference frame. It should be noted that the difference between these reference frames is the rotating speed of the frame, where the speeds are zero (stationary), the

electrical angular speed of the generator's rotor and synchronous of the given frames respectively. To achieve an independent control of the active and reactive power and to simplify the model of DFIG by eliminating the zero sequence components, the direct and quadrature rotating axis reference frame has been frequently implemented to model the DFIG.

C. DQ Reference Frame

Over the course of researching this project, many studies aimed at modeling the DFIG in reference were analyzed [7]. The main differences between the models were the signs. Some were modeled as a general machine (the signs of the currents are identical and indicate that the currents flow towards the machine), unlike Fig.2, while other models were designed as a generator (the signs of the and are opposite, where flows towards the grid) [7] or established as a generator (the signs of the and are similar, where and flow towards the grid), as shown in Fig.1. However, even between [9] and [17] there is a difference, but not in the current signs. Instead, the difference is in the polarity of the voltage, which is induced by a changing flux. Therefore, to find an acceptable model of a DFIG, mathematical and electrical laws have been applied. First, a stator and rotor flux linkage (ψ_s, ψ_r) will be produced by the stator and rotor induced currents (I_s, I_r), respectively. By a change in the flux linkage, the polarity of the induced voltage opposes the current which produces it (Lenz's law). Second, a transformation matrix is applied to the traditional a, b, c model to switch to the dq reference frame. As a result, Figure 4.2 will be devolved to Figure 4.5. Furthermore, from Figure 4.5, it can be observed that, the polarities of the induced voltages which are induced by the change of the flux linkage will oppose the polarities of the I_{dqs} and I_{dqr} , respectively.

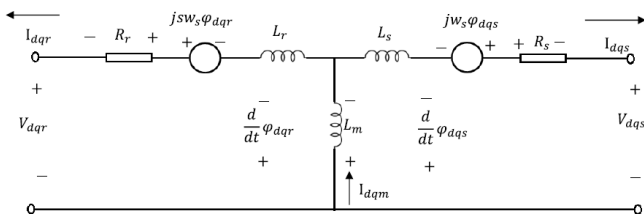


Fig. 4. The dq model of DFIG

Third, applying the Kirchhoff voltage law to Fig.4 will give:

$$v_{dqs} = -I_{dqs}R_s + j\omega_s \phi_{dqs} - \frac{d}{dt} \phi_{dqs} \quad (6)$$

$$v_{dqr} = -I_{dqr}R_r + j\omega_s \phi_{dqr} - \frac{d}{dt} \phi_{dqr} \quad (7)$$

The stator and rotor phase of DFIG in the reference frame can be expressed according to the following equations:

$$v_{ds} = -R_s I_{ds} - \frac{d}{dt} \phi_{ds} - \omega_s \phi_{qs} \quad (8)$$

$$v_{qs} = -R_s I_{qs} - \frac{d}{dt} \phi_{qs} - \omega_s \phi_{ds}$$

$$v_{dr} = -R_r I_{qr} - \frac{d}{dt} \phi_{dr} - (\omega_s - \omega_{gelec}) \phi_{qr} \quad (9)$$

$$v_{qr} = -R_r I_{qr} - \frac{d}{dt} \phi_{qr} - (\omega_s - \omega_{gelec}) \phi_{dr} \quad (10)$$

$$v_{dr} = -R_r I_{qr} - \frac{d}{dt} \phi_{dr} - (\omega_s - \omega_{gelec}) \phi_{qr} \quad (11)$$

Where,

$$\phi_{ds} = L_s I_{ds} + L_m I_{dr} \quad (12)$$

$$\phi_{qs} = L_s I_{qs} + L_m I_{qr} \quad (13)$$

$$\phi_{dr} = L_r I_{dr} + L_m I_{ds} \quad (14)$$

$$\phi_{qr} = L_r I_{qr} + L_m I_{qs} \quad (15)$$

V_{ds}, V_{dr} :d-axis stator voltage and current
 V_{qs}, V_{qr} :q-axis stator voltage and current
 I_{ds}, I_{dr} :d-axis rotor voltage and current
 I_{qs}, I_{qr} :q-axis rotor voltage and current
 Ψ_{ds} :d-axis stator flux linkage
 Ψ_{dr} :d-axis rotor flux linkage
 Ψ_{qs} :q-axis stator flux linkage
 Ψ_{qr} :q-axis rotor flux linkage

It should be noted that Equations (4), (5) represent the DFIG as a fifth-order model. Also, DFIG can be represented as a third-order model when the stator transients (i.e., the differential term in Equations (4) are left out, which increases the computation speed in power system simulation software [17, 20]. In [3], a first-order model was given by leaving out the rotor transient. It should also be mentioned that the demonstrated equation of the DFIG dynamic model (4)(5) are also given in [19].

The active power of the stator P_s , rotor P_r , generated power P_g and electromagnetic torque T_{elec} are calculated as:

$$P_s = \frac{3}{2} (V_{ds} I_{ds} + V_{qs} I_{qs}) \quad (16)$$

$$P_r = \frac{3}{2} (V_{dr} I_{dr} + V_{qr} I_{qr}) \quad (17)$$

$$P_g = P_s + P_r \quad (18)$$

$$T_{elec} = L_m (I_{qs} I_{dr} - I_{ds} I_{qr}) \quad (19)$$

The reactive power of the stator, rotor and generated power are calculated as:

$$Q_s = \frac{3}{2} (V_{qs} I_{ds} + V_{ds} I_{qs}) \quad (20)$$

$$Q_r = \frac{3}{2} (V_{qr} I_{dr} + V_{dr} I_{qr}) \quad (21)$$

$$Q_g = Q_s + Q_r \quad (22)$$

The stator and rotor currents in dq reference frame separately is given for the modeling of DFIG as

$$i_{qs} = \frac{(\varphi_{qs} - \varphi_{mq})}{x_{ls}} \quad (23)$$

$$i_{ds} = \frac{(\varphi_{ds} - \varphi_{md})}{x_{ls}} \quad (24)$$

$$i_{qr} = \frac{(\varphi_{qr} - \varphi_{mq})}{x_{lr}} \quad (25)$$

$$i_{dr} = \frac{(\varphi_{dr} - \varphi_{md})}{x_{lr}} \quad (26)$$

Where φ_{mq} and φ_{md} are useful in representing saturation which are defined as in (14),(15) and (16)

$$\varphi_{mq} = X_{aq} \left(\frac{\varphi_{qs}}{X_{ls}} + \frac{\varphi_{qr}}{X_{lr}} \right) \quad (27)$$

$$\varphi_{md} = X_{ad} \left(\frac{\varphi_{ds}}{X_{ls}} + \frac{\varphi_{dr}}{X_{lr}} \right) \quad (28)$$

$$X_{aq} = X_{ad} = \left(\frac{1}{X_m} + \frac{1}{X_{ls}} + \frac{1}{X_{lr}} \right)^{-1} \quad (29)$$

As the voltage equations in arbitrary reference frame, the flux linkages can be solved by the following integral equations

$$\varphi_{qs} = \frac{\omega b}{p} \left(V_{qs} - \frac{\omega}{\omega b} \varphi_{ds} + \frac{r_s}{X_{ls}} (\varphi_{mq} - \varphi_{qs}) \right) \quad (30)$$

$$\varphi_{ds} = \frac{\omega b}{p} \left(V_{ds} - \frac{\omega}{\omega b} \varphi_{qs} + \frac{r_s}{X_{ls}} (\varphi_{md} - \varphi_{ds}) \right) \quad (31)$$

$$\varphi_{qr} = \frac{\omega b}{p} \left(V_{qr} - \left(\frac{\omega - \omega r}{\omega b} \right) \varphi_{dr} + \frac{r_r}{X_{lr}} (\varphi_{mq} - \varphi_{qr}) \right) \quad (32)$$

$$\varphi_{dr} = \frac{\omega b}{p} \left(V_{dr} - \left(\frac{\omega - \omega r}{\omega b} \right) \varphi_{qr} + \frac{r_r}{X_{lr}} (\varphi_{md} - \varphi_{dr}) \right) \quad (33)$$

The expression used to compute the rotor speed is written as

$$\omega_r = \frac{(T_e - T_l)p}{2j} \quad (34)$$

Where j is the inertia of rotor.

With the help of these equations the DFIG is modeled. For smooth reactive power control, a flexible AC transmission system (FACTS) can be the right option. Different types of FACTS can be used, such as a static synchronous compensator (STATCOM) depending on the desired options when a reactive current supply is required during grid faults [11]. The STATCOM provides reactive power at and supports the grid voltage during voltages drop. Consequently, in this work, the FRT capability of DFIG is studied by utilizing STATCOM controller. The model of STATCOM controllers used in this project is from the MATLAB/SIMULINK library.

III. METHODOLOGY AND MODELING

A. Description Of The System

A one-line diagram of the system is shown in Fig. 5. As we can see, a wind farm of 9MW is connected to a 50Km distribution system. The distribution system is represented by a 25KV, 50Hz, translating power to a grid represented by 120 KV. A step-down transformer 1 25KV/575V and transformer 2 120KV/25KV are applied.

There are five bus bars (B1, B2, B3, B4 and PCC) with voltages 575 V, 25KV, 25KV, 120KV and 120 KV, respectively. As well, load and plant are connected to B1 and B3, respectively.

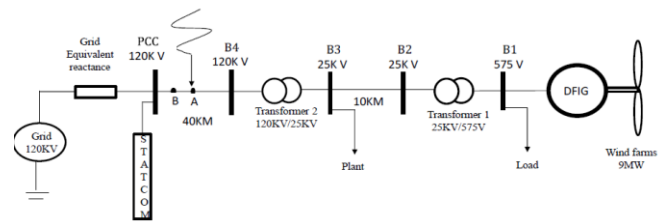


Fig. 5. One-line diagram

B. Modeling of Wind Turbine

In modeling wind turbines, three basic components are taken into consideration: the turbine rotor, the gear box, and the generator shaft and electrical generator. These are defined as aerodynamic, mechanical and electrical components, respectively. The interaction between these three components is shown in Fig. 2. In [23], it was determined that the amount of mechanical power that can be extracted from the wind by a turbine rotor depends on the dynamics of the wind (the aerodynamic component) and the response of wind turbine (the mechanical component). Hence, both the aerodynamic model and the mechanical model are required in wind turbine modeling.

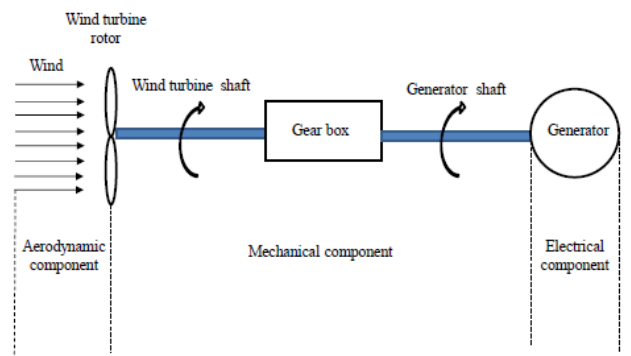


Fig. 6. Basic wind turbine components

1. Aerodynamic Component Model

In a wind turbine simulation with FRT capability, it is desirable to involve the aerodynamic model during grid Disturbances [12]. The aim of this model is to extract mechanical power from the wind by the rotor of the wind

turbine, as mentioned in section 5.2. Eq. 35. is referred to as a mechanical power equation [24, 25]. The magnitude of this equation depends on air density and wind velocity [1]

$$P_{mech} = C_p(\lambda, \beta) \frac{\rho A}{2} V_{wind}^3 \quad (35)$$

- P_{mech} : the mechanical output power extracted from the wind
- C_p : the performance coefficient or the power coefficient
- λ : the tip speed ratio between turbine speed and wind speed
- β : the pitch angle of the rotor blades, deg
- ρ : the air density, Kg/m³
- A : the area covered by rotor blades, m²
- V_{wind}^3 : the wind speed, m/s

The performance coefficient or the power coefficient is considered as a characteristic of wind turbines. However, there are various methods to calculate C_p .

2. Wind Turbine Characteristics

The characteristics of any wind turbine may be defined as, as a function of WT- rotor speed for different wind speeds as well as different pitch angles. Eq. 35 are used for this purpose. A MATLAB program was written to draw the performance coefficient C_p as a function of tip speed ratio (λ), with pitch angle (β) as a parameter. As a result, the C_p (base) and (λ (base) at $\beta=0$ have been calculated as 0.4798 and 8, respectively, as shown in Fig. 7.

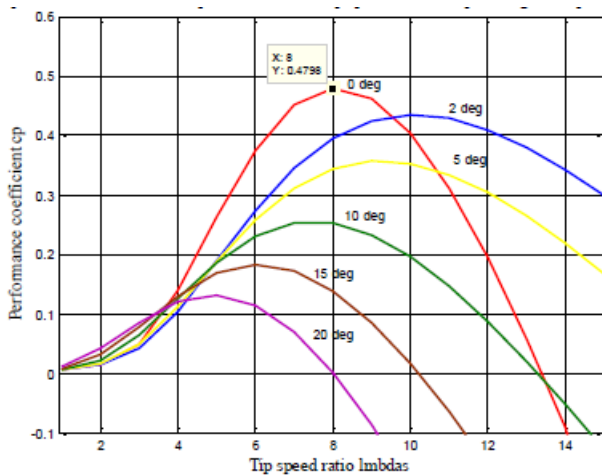


Fig.7. The performance coefficient C_p as a function of tip speed ratio λ , with pitch angle β as a parameter

In this project unlike the conventional simulations which use the wind turbine block in the MATLAB /SIMULINK library, a block was modeled by supplementing the drive train subsystem at 12(m/s) base wind speed, at this base wind speed $K_p = 0.73$ pu, and $Wg_{mech} = 1.2$ (pu) have been implemented using MATLAB /SIMULINK. These values have been taken from [20], for the wind speeds 14, 13.2, 12, 10.8, 9.6, 8.4, 7.2 and 6 m/s. The MATLAB program is written, while the Simulink file is shown in Fig.8 and the wind turbine

characteristics are illustrated in Fig.7. The aim of the characteristics of any wind turbine is to provide an expectation of how to design the generator's control system in order to track these characteristics and extract maximum power from the wind.

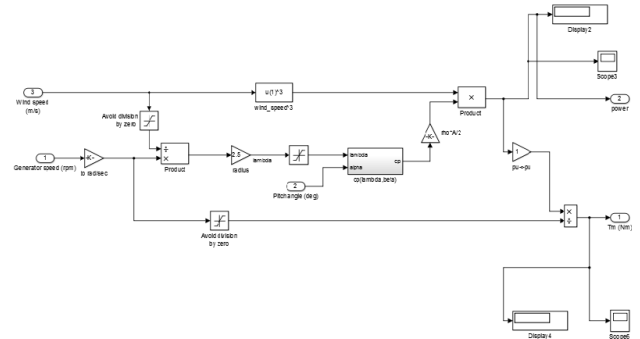


Fig. 8 MATLAB/SIMULINK of a wind turbine

Based on the Eq. 35 the power of the wind turbine is calculated and modeled. With the help of equations the power coefficient and tip speed ratio is calculated in the model of wind turbine.

C. Model of DFIG System

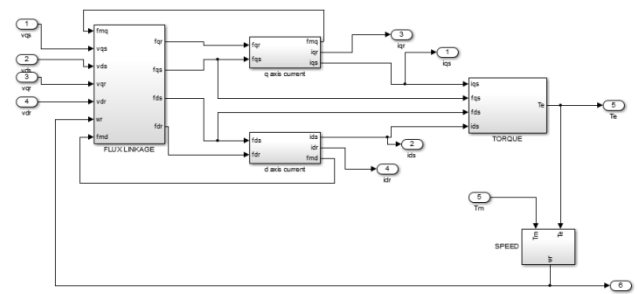


Fig.9. DFIG Simulink Model

With the help of the equations of DFIG described in chapter 4 the modeling of DFIG was carried out. By using the Eq. 17 to Eq. 21 the flux linkages are calculated. Then with the help of calculated flux linkage and Eq.10 to Eq. 16 the stator and rotor current in dq reference frame is modeled. The simulink model in given in Fig. 9. By using Eq. 5 and Eq. 21, the electrical torque and the rotor speed of DFIG is calculated and modeled.

D. MODEL OF PROPOSED SYSTEM

The voltage from the grid is in abc axis is then converted to dq reference frame in terms of stator and rotor voltages and given as the input to the DFIG. Also the mechanical torque obtained from the wind turbine is given as an input to DFIG. The output current, speed, Real and Reactive power obtained from the machine are analyzed under normal and Fault conditions.

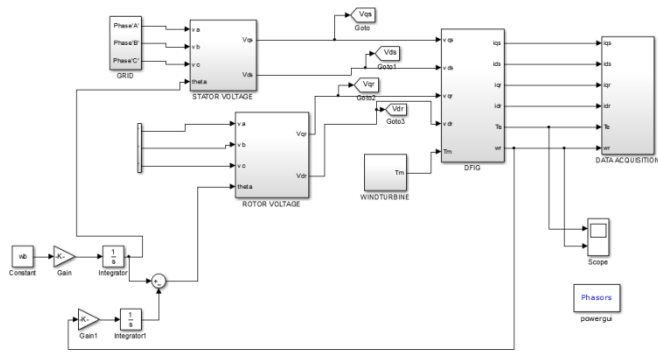


Fig.10. Main Proposed Simulink Diagram

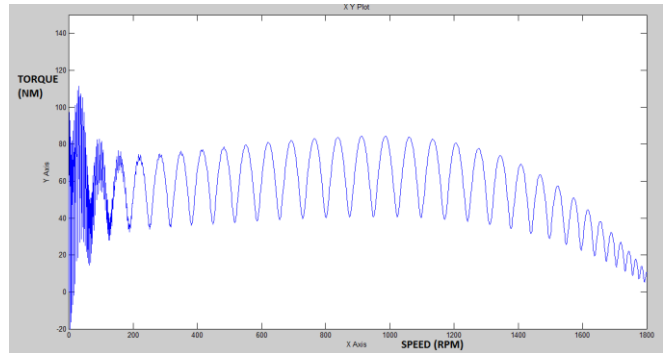


Fig.12 Torque vs Speed Characteristics during fault

E. MODEL OF GRID

A transmission line is modeled representing a 120 KV system. A step-down transformer 1 25KV/575V and transformer 2 120KV/ 25KV are applied, to represent a 25KV 50 Hz system. A Grid with fault in given in Fig 5.7 and a grid with fault and protection using STATCOM controller is given in Fig. 11. The parameters for machine modeling are given in

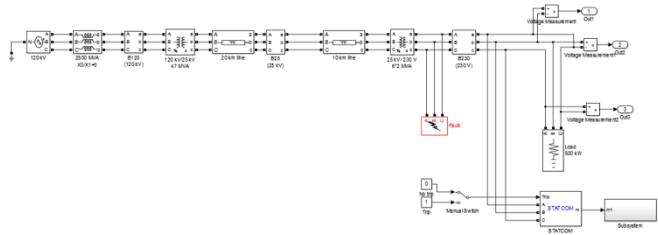


Fig.11. Grid with Fault and protection using STATCOM control

Table 1 represents the characteristics of generator speed with the varying wind velocity accordingly the mechanical torque obtained from wind turbine.

WIND SPEED(m/s)	TORQUE (Tm)	GENERATOR SPEED (SIMULATION)
9	-10.2	1745
12	-11.01	1804
14	-11.9	1835

IV. SIMULATION RESULTS

A. DFIG performance under fault condition

A Single phase fault is applied to the grid. Hence during the fault condition the torque vs speed characteristics is given in Fig. 12. Due to fault, oscillations are found in the characteristic curve.

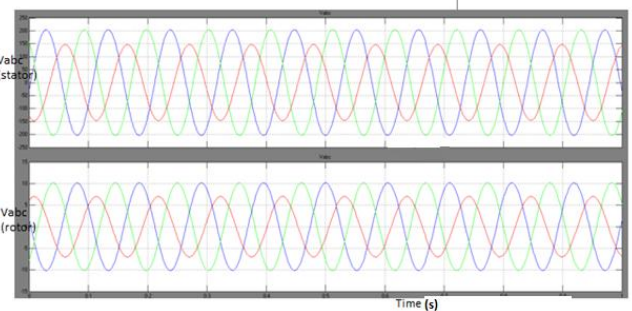


Fig.13. Stator and Rotor Voltage under single phase fault

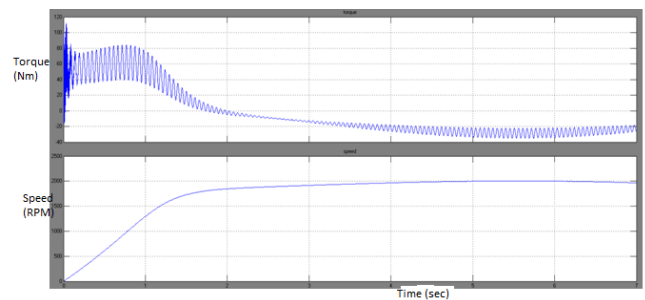


Fig.14. Torque and speed under fault

Similarly during the single phase fault the voltage, torque, speed characteristics are shown in Fig. 13 and 14 respectively. In rotor and stator voltage, the voltage of phase C alone is reduced.

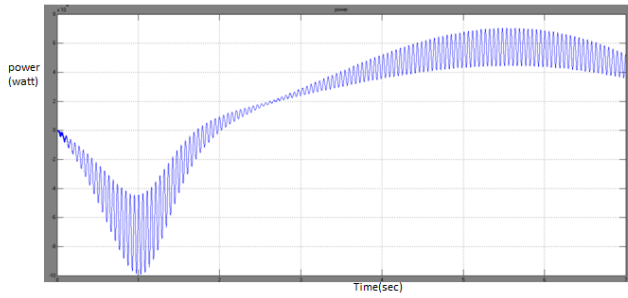


Fig.15. Power curve during fault

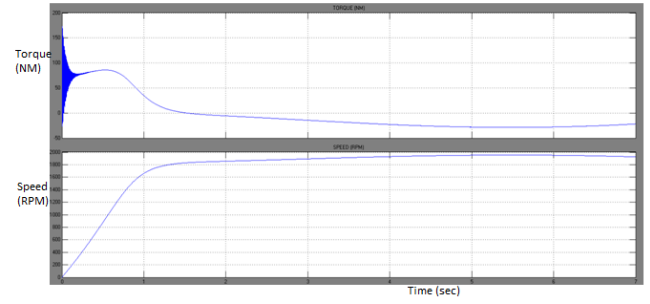


Fig.18 Torque and speed curves

Similarly during the single phase fault the Power, Real and Reactive power characteristics are shown in Fig 14 and 15 respectively. Due to fault, oscillations are found in the power characteristic curve.

Torque and Speed characteristics after the compensation of fault using STATCOM Controller is shown in Fig 17 and 18 respectively.

B. DFIG performance with STATCOM protection

To overcome the fault a STATCOM Controller is used for the protection of DFIG and the compensation of power in the grid. The stator and rotor voltages obtained after the introduction of STATCOM are shown in Fig 16

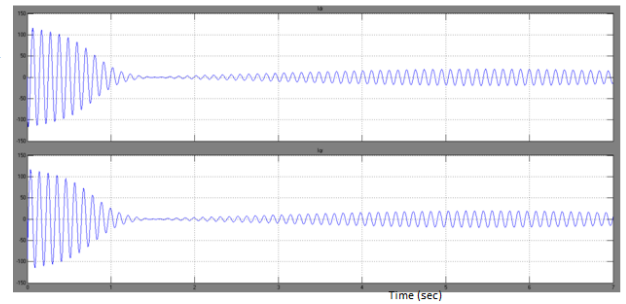


Fig.19 Rotor and Stator Current

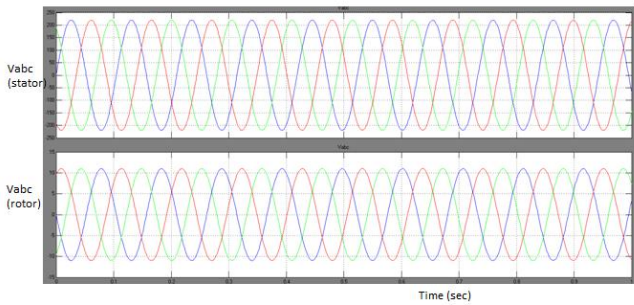


Fig.16 Stator and Rotor Voltage

Fig 19 and 20 represents the rotor, stator currents and power characteristics of DFIG after the compensation of fault using STATCOM controller respectively. The oscillations found in the power characteristic curve are cleared after using the FRT.

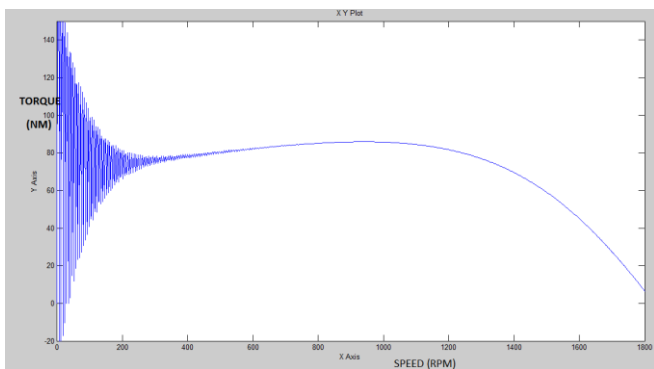


Fig.17 Torque vs Speed Characteristics

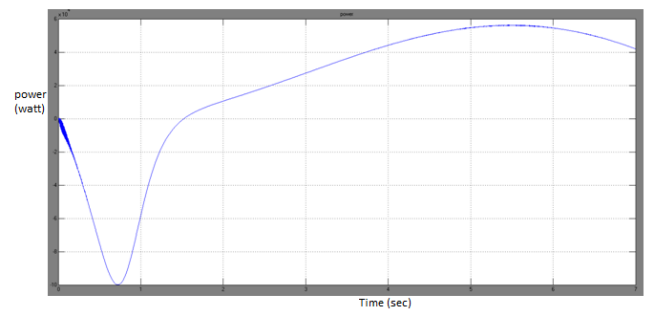


Fig.20 Power characteristics

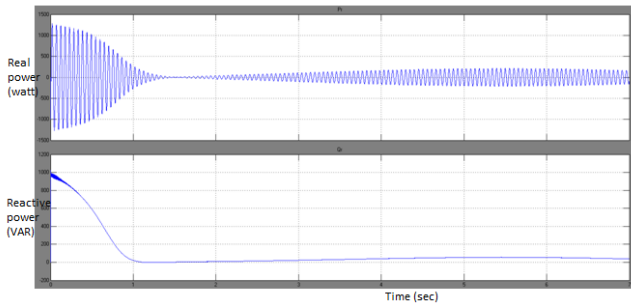


Fig.21 Real and Reactive power

Similarly the real and reactive power after compensation of fault are shown in Fig. 21. Though STATCOM is used for the compensation of power a small lag is there from 1 to 2 seconds which should be overcome in the future work.

V. CONCLUSION

Overcoming limitations and issues related to the FRT capability of the DFIG is currently a prime topic of research, and many techniques have been proposed in this area. In this present work, the FRT issue was enhanced by using the proposed STATCOM controller. Currently, due to increased review in this paper demonstrated the current and past methods used to address and resolve issues related to FRT capability of DFIG wind turbines. The focus of this project is how to improve the FRT in light of the issues discussed in the review. For a fixed wind turbine, there are numerous options for fulfilling the requirements of reactive power, the best one of which uses FACTS controllers. However, for a DFIG coupled to a wind turbine, this compensation can be achieved with the assistance of a back-to-back converter as well FACTS controllers. Simulation results are provided to verify the proposed control approach.

References

- [1] Po-Hsu Huang, Mohamed Shawky El Moursi, Weidong Xiao and James L. Kirtley Jr, "Novel Fault Ride-Through Configuration and Transient Management Scheme for Doubly Fed Induction Generator", *IEEE Trans on Energy conv*, vol. 28, no. 1, Mar. 2013
- [2] S. Zhang, K.-J. Tseng, S. S. Choi, T. D. Nguyen, and D. L. Yao, "Advanced control of series voltage compensation to enhance wind turbine ride through," *IEEE Trans. Power Electron.*, vol. 27, no. 2, pp. 763-772, Feb. 2012
- [3] A. O. Ibrahim, T. H. Nguyen, D.-C. Lee, and S.-C. Kim, "A fault ride through technique of DFIG wind turbine systems using dynamic voltage restorers," *IEEE Trans. Energy Convers.*, vol. 12, no. 3, pp. 871-882, Sep 2011.
- [4] C. Wessels, F. Gebhardt, and F. W. Fuchs, "Fault ride-through of a DFIG wind turbine using a dynamic voltage restorer during symmetrical and asymmetrical grid faults," *IEEE Trans. Power Electron.*, vol. 26, no. 3, pp. 807-815, Mar. 2011.
- [5] D. Ramirez, S. Martinez, C. A. Platero, F. Blazquez, and R. M. de Castro, "Low-voltage ride-through capability for wind generators based on dynamic voltage restorers," *IEEE Trans. Energy Convers.*, vol. 26, no. 1, pp. 195-203, Mar. 2011.
- [6] J. Yang, J. E. Fletcher, and J. O'Reilly, "A series-dynamic-resistor-based converter protection scheme for doubly-fed induction generator various fault conditions," *IEEE Trans. Energy Convers.*, vol. 2 pp. 422-432, Jun. 2010
- [7] L. G. Meegahapola, T. Littler, and D. Flynn, "Decoupled-DFIG fault ride through strategy for enhanced stability performance during grid faults," *IEEE Trans. Sustainable Energy*, vol. 1, no. 3, pp. 152-162, Oct. 2010.
- [8] S. Seman, J. Niiranen, and A. Arkkio, "Ride-through analysis of doubly fed induction wind-power generator under unsymmetrical network disturbance," *IEEE Trans. Power Syst.*, vol. 21, no. 4, pp. 1782-1789, Nov. 2009.
- [9] J. G. Nielsen and F. Blaabjerg, "A detailed comparison of system topologies for dynamic voltage restorers," *IEEE Trans. Ind. Appl.*, vol. 41, no. 5, pp. 1272-1280, Sep./Oct. 2009.
- [10] Jia, X., Tian L., Xing Z. X., Su X. B., "Dynamic Model and Simulation of Double Feed Induction Generator Wind Turbine," *IEEE International Conferences on Automation and Logistics*, pp.1667-1671, 2009.
- [11] A. D. Hansen and G. Michalke. "Fault ride-through capability of DFIG wind turbines." *IEEE Renewable Energy*, vol. 32, no. 9, pp. 1594-1610, 2009.
- [12] K. Ahsanullah and J. Ravishankar, "Fault ride-through of doubly-fed induction generators," in *Proc. of Int. Conference on Power, Signals, Controls and Computation (EPSCICON)*, 2008, pp. 1-6.
- [13] J. G. Nielsen, M. Newman, H. Nielsen, and F. Blaabjerg, "Control and testing of a dynamic voltage restorer (DVR) at medium voltage level," *IEEE Trans. Power Electron.*, vol. 19, no. 3, pp. 806-813, May 2008
- [14] Morren and S. W. H. de Haan, "Ride through of wind turbine doubly-fed induction generator during a voltage dip," *IEEE Trans. Energy Convers.*, vol. 20, no. 2, pp. 435-441, Jun. 2007.
- [15] L. Zhang, X. Jin and L. Zhan. "Reactive power control of doubly fed induction generator during grid voltage dips," in *proc. APPEEC 2012 Power and Energy Engineering Conference*, 2007.
- [16] S. Seman, J. Niiranen and A. Arkkio. "Ride-through analysis of doubly fed induction wind-power generator under unsymmetrical network disturbance." *Power Systems, IEEE Transactions*, vol. 21, no 4, pp. 1782-1789, 2006.
- [17] Dawei Xiang, Li Ran, P. J. Tavner and S. Yang. "Control of a doubly fed induction generator in a wind turbine during grid fault ride-through." *Energy*

- Conversion*, IEEE Transactions, vol. 21,no. 3, pp. 652-662, 2006.
- [18] Jin Yang, J. E. Fletcher and J. O'Reilly. "A series-dynamic-resistor-based converter protection scheme for doubly-fed induction generator during various fault conditions." *Energy Conversion, IEEE Transactions*, vol. 25, no.2 , pp. 422-432,2010.
- [19] B. Gong, D. Xu and B. Wu. "Cost effective method for DFIG fault ride-through during symmetrical voltage dip,"in *proc.IECON 2010,36th Annual Conference on IEEE Industrial Electronics Society*, pp. 3269-3274, 2007.
- [20] C. Zhan and C. D. Barker. "Fault ride-through capability investigation of a doubly-fed induction generator with an additional series-connected voltage source converter. Presented at AC and DC Power Transmission,"in *proc.ACDC 2006, 8th IEE International Conference* , pp.79 -84, 2006.
- [21] J. Morneau, C. Abbey and G. Joos." Effect of low voltage ride through technologies on wind farm,"in *proc.Electrical Power Conference, 2007. EPC 2007. IEEE Canada*, pp.56 -61 ,2006 .
- [22] N. Joshi and N. Mohan. "A novel scheme to connect wind turbines to the power grid. *Energy Conversion, IEEE Transactions*, vol.24, no.2, pp. 504-510,2004.
- [23] S. Santoso and H. T. Le. "Fundamental time-domain wind turbine models for wind power studies," *Renewable Energy*, vol. 32,no. 14, pp. 2436-2452. 2004.
- [24] Heier, Siegfried. *Grid integration of wind energy conversion systems*. Hoboken: Wiley, 1998.